A–dependence in dilepton rapidity distributions: parton model and dipole approach analysis

E.G. de Oliveira

emmanuel.deoliveira@ufrgs.br

High Energy Physics Phenomenology Group
Physics Institute
Universidade Federal do Rio Grande do Sul
Porto Alegre, Brazil

Outline

- Motivation to dilepton production
- Improved parton model
- Color dipole approach
- Dipole cross section
- Nuclear PDFs
- Results
- Summary

Motivation to dilepton production at backward rapidities

- Dilepton $\Rightarrow$ clean probe (electromagnetic interactions).
- Dilepton acts as a reference to hadron probes.
- p–p collisions: no nuclear effects.
- A–A collisions: nuclear effects with the formation of a dense medium.
- p–A collisions: nuclear effects without the formation of a dense medium.
- Furthermore, saturation effects are studied at RHIC and LHC collisions.

We are interested in high density QCD (low-x physics) in high energy hadron collisions.

Motivation to dilepton production at backward rapidities

- p–A is an asymmetrical collision:
- Forward rapidities (proton direction):
  - Overlap in nucleus protons between parton saturation and nuclear effects such as shadowing.
  - High density of partons in the nucleus that can be described by dense systems (such as the Color Glass Condensate);
- Backward rapidities (heavy ion direction):
  - Saturation in the proton.
  - Nuclear effects in the heavy ion.
- Therefore, backward rapidities is complementary in our understanding on nuclear collisions.

We compare how two different models take into account such effects: the improved parton model and the color dipole approach.

Improved parton model

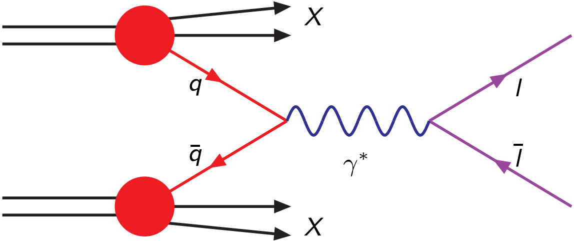

- In the infinite momentum frame (IMF), both hadrons are understood as composed by partons in the Drell–Yan process: Phys. Rev. Lett. 25, 316 (1970); Ann. Phys. 66, 578 (1971).
- In this frame, the process is understood as the combination of two partons to create the virtual photon that splits into the dilepton (ignoring Z.)

Intrinsic transverse momentum

- Partons collinear to hadrons $\Rightarrow$ experimental results of p_T distribution cannot be reproduced for small p_T.
- Introduce (two–dimensional) parton intrinsic transverse momentum G. Altarelli, G. Parisi, and R. Petronzio, Phys. Lett. B76, 351 (1978); Phys. Lett. B76, 356 (1978).
- We use a Gaussian intrinsic k_T distribution of a single parton as given by:

$$\frac{1}{\pi \left\langle k_T^2 \right\rangle} \exp\left(-\frac{k_T^2}{\left\langle k_T^2 \right\rangle}\right)$$

- $\left\langle k_T^2 \right\rangle = \frac{4}{\pi} \left\langle k_T \right\rangle^2$.
- Gaussian distribution of intrinsic k_T due to both partons:

$$h(k_T^2) = \frac{1}{2\pi \left\langle k_T^2 \right\rangle} \exp\left(-\frac{k_T^2}{2\left\langle k_T^2 \right\rangle}\right)$$

- In a NLO study of pion production (P. Levai, G. Papp, G. G. Barnafoldi, and G. I. Fai, Eur. Phys. J. ST 155, 89 (2008)), $\left\langle k_T^2 \right\rangle = 2.5$ GeV was found to reproduce RHIC data even for low p_T.

Improved parton model — Cross section

- The Drell–Yan cross section at NLO is given by:

$$\frac{d\sigma}{dM^2dyd^2p_\mathrm{T}} = h(p_\mathrm{T}^2)\frac{d\sigma}{dM^2dy} + \int d^2k_\mathrm{T}\,\sigma_\mathrm{P}(s,M^2,k_\mathrm{T}^2)\left[h((\mathbf{p}_\mathrm{T}-\mathbf{k}_\mathrm{T})^2)-h(p_\mathrm{T}^2)\right].$$

  R. D. Field, Applications of Perturbative QCD, Addison-Wesley (1989)
  J. Raufeisen, J.-C. Peng, and G. C. Nayak, Phys. Rev. D66, 034024 (2002)

- NLO collinear double differential cross section $d\sigma/dM^2dy$ (no p_T dependence).
- Together with $h(p_\mathrm{T}^2)$, Gaussian dependence on p_T.
- This p_T dependence is completely factorized.
- The first term is dominant at small $p_\mathrm{T}/\langle k_\mathrm{T}\rangle$, while the second at high $p_\mathrm{T}/\langle k_\mathrm{T}\rangle$.

Improved parton model — Cross section

- Only noncollinear subprocesses contribute to the second term: Compton scattering $q+g \to q+\gamma^*$ and annihilation $q+\bar{q} \to g+\gamma^*$.
- We have (R. D. Field, Applications of Perturbative QCD):

$$\sigma_{\mathrm{P}}(s, M^2, p_{\mathrm{T}}^2) = \frac{1}{\pi^2}\frac{\alpha^2\alpha_s}{M^2\hat{s}^2}\int_{x_{A\mathrm{min}}}^{1} dx_A \frac{x_B x_A}{x_A - x_1}\left\{P_{q\bar{q}}(x_A, x_B, M^2)\frac{8}{27}\frac{2M^2\hat{s}+\hat{u}^2+\hat{t}^2}{\hat{t}\hat{u}}\right.$$
$$\left. + P_{qg}(x_A, x_B, M^2)\frac{1}{9}\frac{2M^2\hat{u}+\hat{s}^2+\hat{t}^2}{-\hat{s}\hat{t}} + P_{gq}(x_A, x_B, M^2)\frac{1}{9}\frac{2M^2\hat{t}+\hat{s}^2+\hat{u}^2}{-\hat{s}\hat{u}}\right\}.$$

- $x_{1,2} = \sqrt{\frac{M^2+p_{\mathrm{T}}^2}{s}}\mathrm{e}^{\pm y}$, in which y is the virtual photon rapidity.
- Subprocess Mandelstam variables: $\hat{s} = x_A x_B s$, $\hat{t} = M^2 - x_A x_2 s$, and $\hat{u} = M^2 - x_B x_1 s$.
- Parton momentum fractions: x_A and $x_B = (x_A x_2 - M^2/s)/(x_A - x_1)$.
- The integration lower limit is $x_{A\mathrm{min}} = (x_1 - M^2/s)/(1 - x_2)$.

Improved parton model and PDFs

- The functions $P_{q\bar{q},qg,gq}$ depend on the parton distribution functions:

$$P_{q\bar{q}}(x_A, x_B, M^2) = \sum_q e_q^2 \left(f_q(x_A) f_{\bar{q}}(x_B) + \bar{q} \leftrightarrow q\right)$$

$$P_{qg}(x_A, x_B, M^2) = \sum_q e_q^2 \left(f_q(x_A) + f_{\bar{q}}(x_A)\right) f_g(x_B)$$

$$P_{gq}(x_A, x_B, M^2) = \sum_q e_q^2 f_g(x_A) \left(f_q(x_B) + f_{\bar{q}}(x_B)\right).$$

- PDF parameterizations are needed.
- When it is the case, nuclear PDF parameterizations are used for the B hadron.

Color dipole approach

- In the color dipole approach, the same Drell–Yan process is studied in the target rest frame.
- At backward rapidities, the proton is the target and the nucleus is the projectile. M.A. Betemps, MBGD, E.G. de Oliveira; PRD **74** (2006) 094010
- Two diagrams are involved:

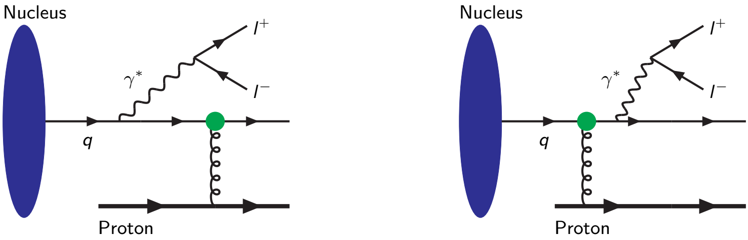

Color dipole approach — Cross section

- The Drell–Yan cross section in the color dipole picture arises as the interference of two diagrams:

$$\frac{d\sigma^{DY}}{dM^2 dy d^2 p_T} = \frac{\alpha_{em}^2}{6\pi^3 M^2} \int_0^\infty d\rho W(x_2, \rho, p_T) \sigma_{dip}(x_1, \rho),$$

- $\sigma_{dip}(x_1, \rho)$ is the dipole cross section and ρ is dipole size.
- The approach is phenomenologically valid for very backward rapidities y, i.e., small $x_1 = \sqrt{\frac{M^2 + p_T^2}{s}} e^y$.
- x_2/A is the projectile momentum fraction carried by photon.
- $x_2/A/\alpha > x_2/A$ is the projectile momentum fraction carried by the projectile parton.
- α is the parton momentum fraction carried by the photon.

Dipole cross section — Cross section

- $W(x_2, \rho, p_T)$ is the weight function and depends on the projectile composition.
- It weights each ρ-sized dipole contribution to the cross section:

$$W(x_2,\rho,p_T) = \sum_q \int_{x_2}^{1} \frac{d\alpha}{\alpha^2} e_q^2 \left[\frac{x_2}{\alpha} f_q^A\left(\frac{x_2}{\alpha}, M^2\right) + \frac{x_2}{\alpha} f_{\bar{q}}^A\left(\frac{x_2}{\alpha}, M^2\right)\right]$$
$$\times \left\{ [m_q^2\alpha^4 + 2M^2(1-\alpha)^2]\left[\frac{1}{p_T^2+\eta_q^2} T_1(\rho) - \frac{1}{4\eta_q} T_2(\rho)\right] \right.$$
$$\left. + [1+(1-\alpha)^2]\left[\frac{\eta_q p_T}{p_T^2+\eta_q^2} T_3(\rho) - \frac{1}{2} T_1(\rho) + \frac{\eta_q}{4} T_2(\rho)\right]\right\},$$

- with $\eta_q^2 = (1-\alpha)M^2 + \alpha^2 m_q^2$ and:

$$T_1(\rho) = \frac{\rho}{\alpha} J_0\left(\frac{p_T\rho}{\alpha}\right) K_0\left(\frac{\eta\rho}{\alpha}\right)$$
$$T_2(\rho) = \frac{\rho^2}{\alpha^2} J_0\left(\frac{p_T\rho}{\alpha}\right) K_1\left(\frac{\eta\rho}{\alpha}\right)$$
$$T_3(\rho) = \frac{\rho}{\alpha} J_1\left(\frac{p_T\rho}{\alpha}\right) K_1\left(\frac{\eta\rho}{\alpha}\right).$$

Dipole cross section

- Dipole cross section in DIS is the cross section between the color dipole component of the virtual photon and the target.
- Golec–Biernat and Wüsthoff modeled Phys. Rev. D59, 014017 (1999) the dipole cross section data as:

$$\sigma_{\mathrm{dip}}(x, r) = \sigma_0 \left[1 - \exp\left(-\frac{1}{4} r^2 Q_s^2(x) \right) \right],$$

  with:

$$Q_s^2(x) = Q_0^2 \left(\frac{x_0}{x} \right)^{\lambda/2} \qquad Q_0^2 = 1\mathrm{GeV}^2.$$

- A recent fit (H. Kowalski, L. Motyka, and G. Watt, Phys. Rev. D74, 074016 (2006)) to DIS data found $\sigma_0 = 23.9$ mb ($61.38\ \mathrm{GeV}^{-2}$), $x_0 = 1.11 \times 10^{-4}$, and $\lambda = 0.287$.
- The model reproduces color transparency for small r ($\sigma_{\mathrm{dip}}(x, r) \propto r^2$ and saturation for large r ($\sigma_{\mathrm{dip}}(x, r) \approx \sigma_0$).
- The property of $\sigma_{\mathrm{dip}}(x, r) = \sigma_{\mathrm{dip}}(rQ_s(x))$ leads the DIS cross section for small x to depend only on $Q/Q_s(x)$ and is called geometric scaling.

Dipole cross section

- Two recently proposed models of our interest:
  - DHJ Dumitru, Hayashigaki, and Jalilian-Marian, Nucl. Phys. A765, 464 (2006); Nucl. Phys. A770, 57 (2006);
  - BUW Boer, Utermann, and Wessels, Phys. Rev. D77, 054014 (2008).
- Both models were used to fit forward d–Au RHIC hadron production data in the context of the Color Glass Condensate.
- The original dipole scattering amplitudes represent quark and gluon interactions with the medium.
- They can be rewritten to represent a dipole cross section.
- Both models start with the following expression:

$$\sigma_{\rm dip}(x,r) = \sigma_0 N_\gamma = \sigma_0 \left[1 - \exp\left(-\frac{1}{4}(r^2 Q_s^2)^{\gamma(M,x)}\right)\right]$$

- If $\gamma(M,x)$ is set to 1, BUW and DHJ models reduce to the GBW model with parameters $\sigma_0 = 23$ mb ($59.07\ \mathrm{GeV}^{-2}$), $x_0 = 3\times10^{-4}$, and $\lambda = 0.3$.

Dipole cross section — DHJ

- In DHJ model the anomalous dimension reads:

$$\gamma(M,x) = \gamma_s + (1-\gamma_s)\frac{|\log(M^2/Q_s^2)|}{\lambda Y + d\sqrt{Y} + |\log(M^2/Q_s^2)|},$$

  with $Y = \log 1/x$ and $\gamma_s = 0.628$.
- The parameter $d = 1.2$ was fitted to data.
- The additional dependence on x not through M^2/Q_s^2 breaks the geometric scaling.
- It is not possible to observe geometric scaling directly from hadron collision data (the opposite is truth in the case of DIS).
- Therefore, one can ask: geometric scaling is needed to describe hadron collision data?

Dipole cross section — BUW

- Recently proposed by Boer, Utermann, and Wessels Phys. Rev. D77, 054014 (2008), BUW model makes the anomalous dimension do not depend on x separately, but only on the variable $w = \sqrt{M^2/Q_s^2(x)}$:

$$\gamma(w) = \gamma_s + (1-\gamma_s)\frac{w^a - 1}{(w^a - 1) + b}.$$

- The best BUW fit to the data gives $a = 2.82$ and $b = 168$.
- Both models were used to fit forward d–Au RHIC hadron production data, the difference being that DHJ violates geometric scaling, while BUW does not.
- Both DHJ and BUW model can explain RHIC results at small x, but at larger x DHJ model deviates from data.
- At LHC energies, the predictions differ even at small x.

Dipole cross section — Comparison

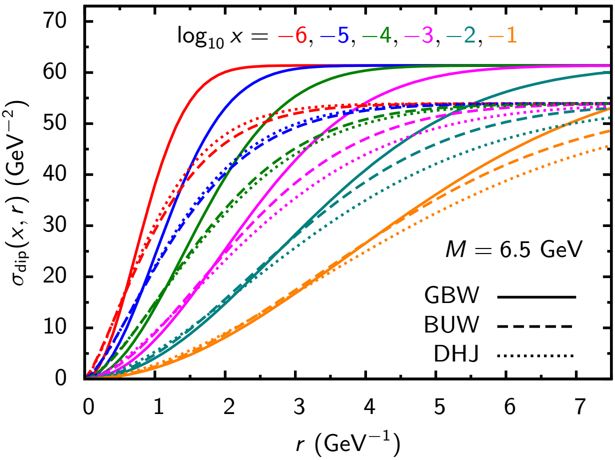

- BUW and DHJ share some similarity for small dipole sizes.

Nuclear PDFs

- Three parameterizations of the nuclear PDFs are used:
  - EKS Nucl. Phys. B535, 351 (1998); Eur. Phys. J. C9, 61 (1999); JHEP 05, 002 (2007)
  - EPS08 JHEP 07, 102 (2008)
  - EPS09 JHEP 04, 065 (2009)
- The parameterizations give the nuclear proton PDF as the free proton PDF multiplied by a factor: $f_q^{\text{proton}-A}(x,Q) = R_q^A(x,Q) f_q^p(x,Q)$.
- To obtain the nuclear neutron PDF, one relies on the isospin symmetry: $f_q^{\text{neutron}-A}(x,Q) = R_{q'}^A(x,Q) f_{q'}^p(x,Q)$; where, if q is up (or down), q' is down (or up).
- For example, the normalized total up distribution in a nucleus is

$$f_u^A = \frac{Z}{A} R_u^A(x,Q) f_u^p(x,Q) + \frac{A-Z}{A} R_d^A(x,Q) f_d^p(x,Q).$$

Nuclear PDF parameterizations

EKS	EPS08	EPS09
LO	LO	NLO (and LO)
Deep inelastic lepton-nucleus scattering and Drell–Yan dilepton production data	Deep inelastic lepton-nucleus scattering and Drell–Yan dilepton production data + RHIC BRAHMS inclusive high-p_T hadron production at high rapidities ($x \approx 10^{-4}$)	Deep inelastic lepton-nucleus scattering and Drell–Yan dilepton production data + RHIC PHENIX inclusive pion production at mid rapidities ($x \approx 10^{-2}$)

- The authors of EPS09 did not use BRAHMS data because they concluded that baseline p–p predictions were not accurate enough.
- As free proton PDF parameterization, we use CTEQ6.1.

Nuclear PDFs — up quark

- R_{UV} and R_{US}: factors of valence and sea up quark.
- Nuclear effects:
  - shadowing ($x \lessapprox 0.01$),
  - antishadowing ($0.01 \lessapprox x \lessapprox 0.3$),
  - EMC effect ($0.3 \lessapprox x \lessapprox 1$), and
  - Fermi motion ($x \approx 1$).
- Stronger shadowing in EPS08.
- EPS09_LO very similar to EKS.

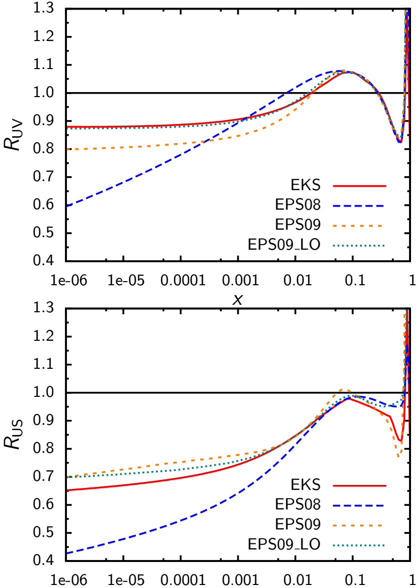

Nuclear PDFs — strange quark and gluon

- R_{SS} and R_{GL}: factors of strange quark and gluon.
- EPS08 shows a very strong shadowing.
- EPS09 shows the weakest shadowing.
- EPS09_LO very similar to EKS.

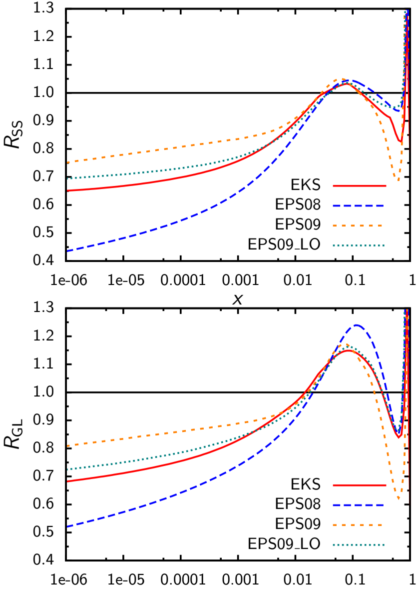

Results

- Dilepton mass of 6.5 GeV.
- RHIC p–p and d–Au collisions at 200 GeV.
- LHC p–p and p–Pb collisions at 8.8 TeV.
- The nuclear modification factor is given by:

$$R_{\mathrm{pA}} = \frac{d\sigma(\mathrm{pA})}{dp_{\mathrm{T}}^2\,dy\,dM} \bigg/ A\,\frac{d\sigma(\mathrm{pp})}{dp_{\mathrm{T}}^2\,dy\,dM}.$$

- If there were no nuclear effects, $R_{\mathrm{pA}} = 1$.
- Therefore, the nuclear modification factor tells how different is a collision between two free protons from a collision of a free proton and a bound nucleon.
- In the case of d–A collisions, deuteron nuclear effects are neglected and the ratio is divided by two times A instead of only A.

Results — p–p cross section (RHIC)

- Cross sections for RHIC p–p collisions at 200 GeV.
- Some disagreement among the σ_{dip} is seen, specially at high p_T, when larger dipole sizes become important.
- $\langle k_T^2 \rangle = 0.5, 2.5$ GeV^2.
- The effects of intrinsic k_T are easily seen.
- Cross sections are prone to variation as $\langle k_T \rangle$ and σ_{dip} change.

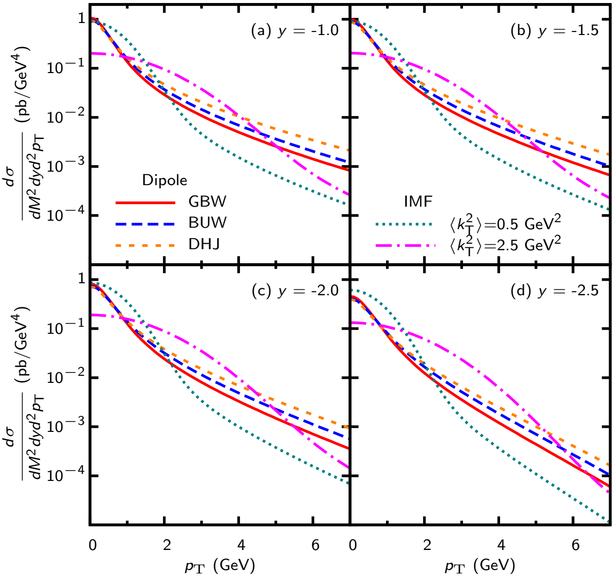

Results — R_{pA} (RHIC)

- R_{dA} for RHIC d–Au collisions at 200 GeV.
- Nuclear effects seen: antishadowing and EMC effect.
- Nuclear effects are very dependent on the intrinsic k_{T}.
- At high $p_{\mathrm{T}}/\langle k_{\mathrm{T}}\rangle$, dipole approach and the IMF agree, since intrinsic k_{T} plays a minor role. (Compton scattering is the dominant subprocess.)
- EPS09 and EPS08 show good agreement.

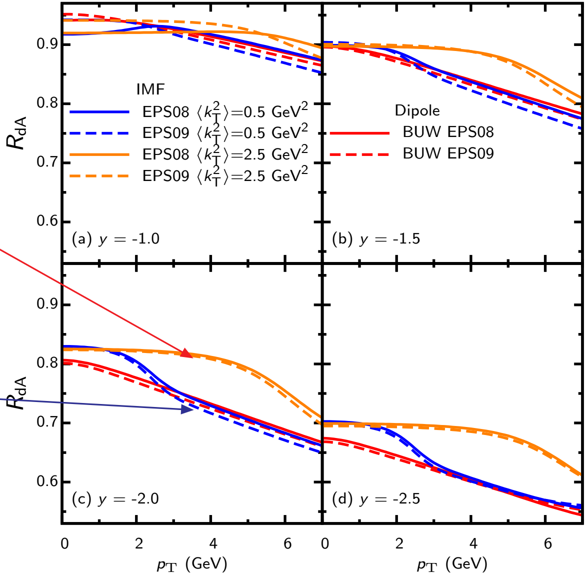

Results — GBW, BUW, and DHJ comparison

- R_{dA} for RHIC d–Au collisions at 200 GeV.
- Only dipole approach.
- GBW, BUW, and DHJ comparison.
- Nuclear effects in these results do not distinguish among dipole cross section parameterizations.
- This despite p–p cross section differences.

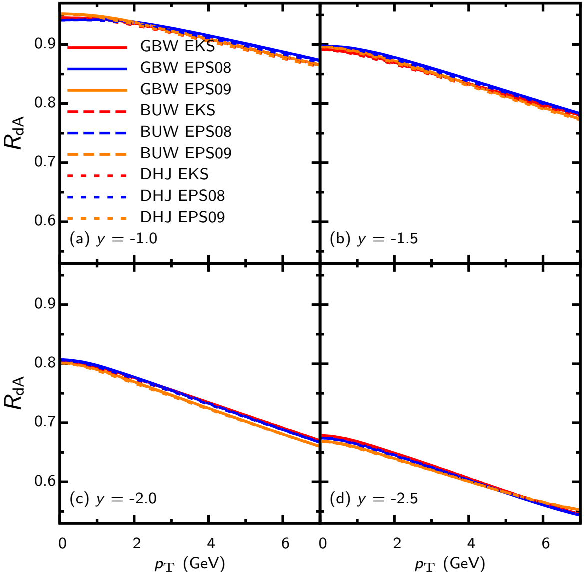

Results — EPS09 and EKS comparison

- R_{dA} for RHIC d–Au collisions at 200 GeV.
- EPS09 and EKS comparison.
- Both nPDFs give approximately the same results.

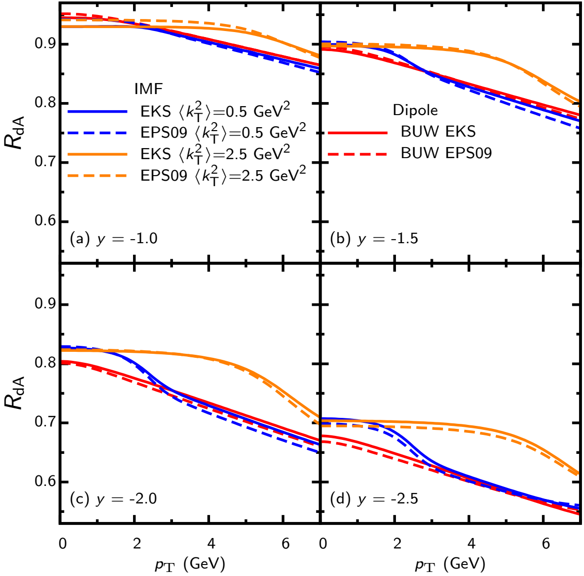

Results — p–p cross section (LHC)

- Cross sections for LHC p–p collisions at 8800 GeV.
- $\sigma_{\rm dip}$ DHJ and BUW models agree, while they disagree with GBW.
- $\langle k_T^2 \rangle = 0.5, 2.0, 4.5$ GeV^2.
- Again, important effects due to intrinsic k_T.
- Again, cross sections are subject to variation as $\langle k_T \rangle$ and $\sigma_{\rm dip}$ change.

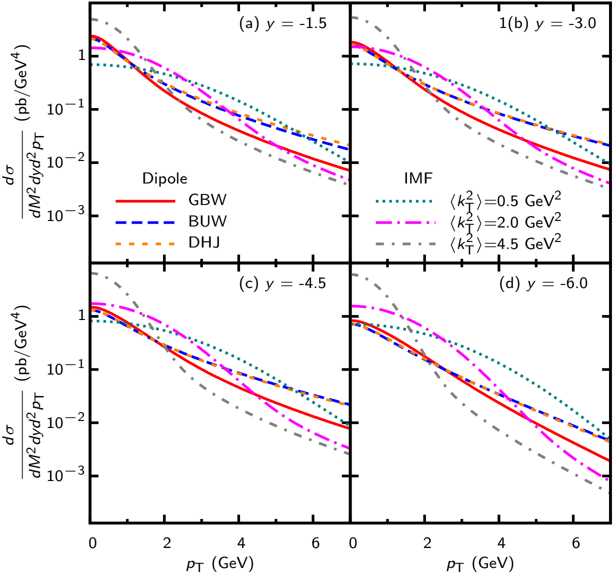

Results — R_{pA} (LHC)

- R_{pA} for LHC p–Pb collisions at 8800 GeV.
- Nuclear effects seen: shadowing, antishadowing, and EMC effect.
- EPS09 and EKS have good agreement, as well as GBW, BUW, and DHJ have (not shown here).
- EPS08 and EPS09 disagree when shadowing is important.
- Again, nuclear effects are very dependent on the intrinsic k_T.
- Dipole approach and the IMF agree at high $p_T/\langle k_T\rangle$.

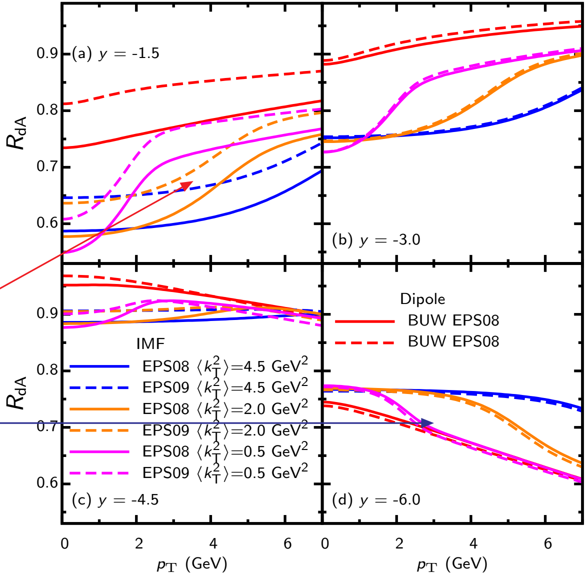

Results — Backward and forward rapidities (RHIC)

- CGC results at forward rapidities at RHIC energies (M. A. Betemps and M. B. Gay Ducati, Phys. Rev. D70, 116005).
- The three ways to calculate the dilepton production agree pretty well; even the transverse momentum dependence is the same.
- Forward rapidities: R_{pA} increases with p_T, due to a necessary increase in the parton momentum fraction, reducing the effect of shadowing.
- At backward rapidities, there is no shadowing but the antishadowing effect, leading to a decrease of R_{pA} with p_T.

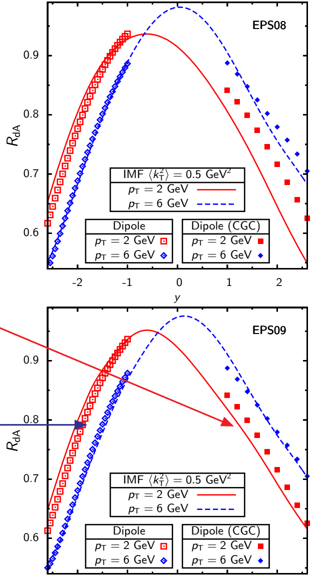

Results — Backward and forward rapidities (LHC)

- At LHC energies, forward rapidity results disagree.
- Only the qualitative p_T dependence is kept.
- From mid to forward rapidities, less annihilation and more Compton scattering subprocess become important.
- EPS09 has an increase at forward rapidities as y increases.
- This happens because quark shadowing is stronger than gluon shadowing and shadowing is not sufficiently enhanced as $x \to 0$.
- In EPS08, shadowing is enhanced very fast, therefore the nuclear modification factor always decreases for $y > 0$.

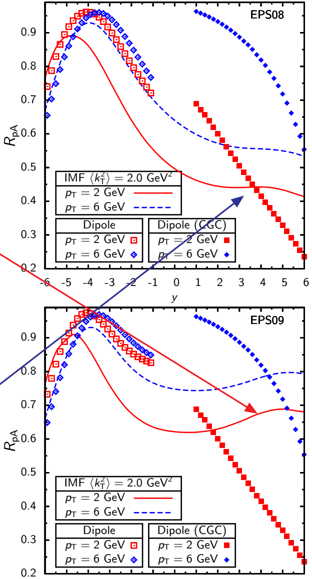

Summary

We studied the nuclear effects in the improved parton model and the color dipole approach through the nuclear modification factor.

- Nuclear effects at y are not sensitive to different dipole cross sections (no hint about geometric scaling).
- Introduction of the intrinsic transverse momentum can change R_{pA} of ≈ 0.1.
- Color dipole approach misses the changes in nuclear effects due to intrinsic k_{T}.
- At RHIC, different models qualitatively agree.
- At LHC, forward models qualitatively disagree due to the interplay of quark and of gluon shadowing.

Dileptons bring a lot of information on nuclear effects.